Quantifying photosynthetic restrictions

Chandra Bellasio

Laboratory of Theoretical and Applied Crop Ecophysiology, School of Biology & Environmental Science, University College Dublin, Belfield, Dublin 4, Dublin; Biology of plants under Mediterranean conditions; Department of Chemistry, Biology and Biotechnology, Università Degli Studi di Perugia, Perugia, 06123, Italy; Department of Biology, University of the Balearic Islands 07122 Palma, Illes Balears, Spain; Research School of Biology, The Australian National University, Acton, ACT, 2601 Australia. ORCID: 0000-0002-3865-7521. chandra.bellasio@ucd.ie

Keywords

Modelling; partitioning; contribution; limitation; control, sensitivity; stomatal; non-stomatal; mesophyll; biochemical, non-diffusional

Abstract

Quantifying the effect of factors controlling CO_2 assimilation is crucial for understanding plant functions and developing strategies to improve productivity. Methods exist in numerous variants and produce various indicators, such as limitations, contributions, and sensitivity, often causing confusion. Simplifications and common mistakes lead to overrating the importance of diffusion – whether across stomata or the mesophyll. This work develops a consistent set of definitions that integrates all previous methods, offering a generalised framework for quantifying restrictions. Ten worked examples are provided in a free downloadable spreadsheet, demonstrating the simplicity and applicability to a wide range of questions.

Introduction

Photosynthetic gas exchange routines measure CO_2 uptake (assimilation, A) and water vapour release (transpiration, E), under a range of external CO_2 concentration and light intensities (Busch et al. 2024). Raw data is first processed by the gas analyser software, to derive stomatal conductance to CO_2 (g_S), together with the CO_2 concentration in the substomatal cavity (C_i) using mass-balance and diffusion theory (von Caemmerer and Farquhar 1981). The resulting ordered pairs (C_i, A) can be described by mathematical models of photosynthesis. These are typically adjusted to match data through curve fitting procedures, which return parameters that capture physical or biochemical characteristics of leaves (Bellasio et al. 2016b; Bellasio et al. 2016a).

A variety of models exist that are typically classified as mechanistic or empirical. In mechanistic models, expressions describe biochemical processes known to occur within leaves; in empirical models, expressions describe the relationship between data patterns. The distinction is merely artificial, because mechanistic models still rely on data, while empirical models describe patterns

that ultimately depend on the same underlying processes. Mechanistic models are typically validated by direct measurements of physical or biochemical properties, and are modular (they can be modified to include more processes, and the description of processes can be refined to virtually any desired level of detail), allowing to accommodate a virtually unlimited range of real or hypothetical scenarios. Empirical models are generally simple, and may become unreliable when used in environmental conditions differing from those under which they were calibrated, but are typically more accurate for describing empirical datasets and valid for all photosynthetic types.

Additional analyses can quantify how physical or biochemical properties, or their experimental manipulation, may restrict assimilation. Restriction analyses seek to gain insights into the state of the assimilation process, rather than estimating the quantities defining it. Various methods based on different assumptions and conventions abound in the literature, and the lack of an objective criterion for their selection often renders the choice of methods "*to some extent arbitrary*" (Jones 1985). The aim of this study is to establish a framework with general validity that is straightforward to implement and unambiguous.

The theoretical basis of restriction analysis were laid by Gaastra (1959). Early studies made the erroneous assumption that CO_2 concentration at the mesophyll carboxylating sites (C_M) is zero. In the 1970s, biochemical CO_2 uptake was treated as a linear function akin to Ohm's Law of electrical resistance (Jarvis 1971; Jones 1973; Jones and Slatyer 1972; Prioul and Chartier 1977). This "*linear resistance analysis is in most cases invalid"* (Farquhar and Sharkey 1982) because photosynthesis typically responds non-linearly with a saturating response to CO_2. In addition, rather than conveying information about the process, resistance confounds with a physical characteristic, making it difficult to relate to the sought process information. Consequently, I deem these methods undesirable and I will not address them further.

The concept of restriction can be related to that of mathematical sensitivity, for review see Jones (1985). Absolute and relative sensitivity (elasticity) quantify the extent to which various input variables (such as C_i) exert control over the process of assimilation. Control analyses have the benefit that, once model parameterization is defined, outputs are unequivocal (Jones 1973). The drawback is that control coefficients are relatively complex to derive, often difficult relate to actual physiological phenomena, and are applicable only to infinitesimal change.

Extending sensitivity analysis to finite changes between two well-identifiable conditions of interest, for instance resulting from experimental manipulation, approximates the response of assimilation to CO_2 concentration at the mesophyll carboxylating sites (A/C_M curve) with a straight line. This practice, which has been widely used both for C_3 plants (Grassi and Magnani 2005) and in its C_4 variant (Cano et al. 2019) introduces error (Deans et al. 2019) and is fundamentally mistaken (Buckley and Diaz-Espejo 2015). The solution proposed by Prioul et al. (1984) was to approximate the A/C_M curve with many small steps; however, the need to derive assimilation graphically and to process data manually, meant that most studies calculated assimilation in only

three points. This raised another issue that the order in which these points are evaluated influences the result of the analysis (path dependency).

Recent key advancements in restriction analysis have been switching from a graphical to a computerised method where drawn curves were replaced by fitted empirical models (Bellasio et al. 2016b). That approach was later utilized to compare C_4 and C_3 plants but remained limited, as it still used the classical three-point calculation, and was only applied to stomatal and non-stomatal limitations (Bellasio et al. 2018). Buckley and Diaz-Espejo (2015) developed over the intuition of Prioul et al. (1984) by increasing the number of steps to any large number of infinitesimal transitions. Their method had the main benefits of being unambiguous, avoiding linearization of assimilatory responses over finite intervals, and implicitly containing sensitivity, thereby reconciling contribution with control analysis. However, it only applied to contribution analysis in C_3 plants, leaving the need for a method that is universally applicable.

This study develops a unified theory and terminology that can be used to analyse controls, limitations and contributions in all plants, and shows the implementation of common procedures in spreadsheets freely available for download, demonstrating the framework's simplicity and applicability to a wide range of questions.

Theory: constructing a general framework

A first common approach called 'limitation analysis' involves comparing a healthy plant with its potential attainable under idealized conditions. The analysis quantifies the gain in assimilation achieved by sequentially 'lifting' limitations until photosynthesis reaches its maximum 'limit'. Hypothesize a healthy plant photosynthesizing under ordinary operational conditions (Figure 1a). Limitation analysis simulates a transition along a hypothetical dimension that lifts all restrictions (number 1 in Figure 1a).

An alternative approach called 'contribution analysis' compares a healthy plant with the same or a similar plant after the imposition of a treatment. The analysis attributes the changes in assimilation to the various quantities responsible for causing the change, that is, 'contributing' to that change in assimilation. Consider, for instance, a set of plants subjected to a generic treatment and left to photosynthesize under the same ordinary operational conditions as the healthy plants. Contribution analysis simulates the effect of the treatment, assigning the change in assimilation to the drivers causing it (number 2 in Figure 1a).

The strength of this new generalised framework lies in its ability to combine restriction analyses in any nuance. The extent to which treated plants are limited under ordinary conditions relative to their maximum limit, can be quantified through a limitation analysis (number 3 in Figure 1a). Any residual difference between the potential of the treated plant and that of the healthy plant can be evaluated through an idealised transition that reverts the treatment (number 4 in Figure 1a). Analyses can also be combined. For instance, in a time-course experiment where a plant undergoes

progressive treatment and is sampled at subsequent time points, limitation analysis can be performed at each time point, while contribution analysis can be used to compare these subsequent time points. Control analysis can be overlaid at any given intermediate point along transitions (a 'C' in Figure 1a) to determine the extent to which an infinitesimal change in the transition is controlled by environmental drivers and the underpinning photosynthetic characteristics.

To formalize this framework, it is necessary to assume that photosynthesis can be described mathematically. Let the function *f* be a set of expressions describing the dependence of any generic output variable Ω on a set of inputs, which are termed *a* (a generic input) and ***b*** (the set of all other inputs):

$$\Omega = f(a, \boldsymbol{b}) \qquad 1$$

This is exemplified by the red line in Figure 2, which plots the values of Ω on the ordinate as a function of *a* on the abscissa, obtained for the specific input set $\boldsymbol{b}_{\mathrm{I}}$ (parameterization). Any situation with well-defined conditions, where *a* and ***b*** are known, will be referred to as a 'state'. These may be the healthy and treatment operational conditions, or the hypothetical scenarios in which limitations are lifted. Only a few states are typically of interest, but, let the number of states be any integer *M*, with *m* being any generic state counted in Roman numbers ($m = \mathrm{I}, \mathrm{II}, \mathrm{III} \ldots . M$).

Any transition between two states is divided in a number of intervals *K*, being the total number of intervals, with *k* being any generic intermediate interval counted in integers ($k = 0, 1, 2, 3 \ldots . K$). In Figure 2, the transition between state I and state II is divided in *K* = 4 intervals.

Following Buckley and Diaz-Espejo (2015) the value of a generic input in the interval *k* scales linearly between the values in the two adjacent known states *m* and *m*+I as:

$$a_{\mathrm{m,k}} = a_{\mathrm{m}} + \frac{k}{K}(a_{\mathrm{m+I}} - a_{\mathrm{m}}), \qquad 2$$

and the calculation is analogous for all other inputs in the set ***b***.

Within the interval *k* to *k*+1 the 'marginal contribution of *a* to the change in Ω' is defined as:

$$\xi(a)_{\Omega} = f\left(a_{\mathrm{m,k+1}}, \boldsymbol{b}_{\mathrm{m,k}}\right) - f\left(a_{\mathrm{m,k}}, \boldsymbol{b}_{\mathrm{m,k}}\right), \qquad 3$$

and is visualised in Figure 2 for the transition from $a_{\mathrm{I},2}$ to $a_{\mathrm{I},3}$. This definition of marginal contribution corresponds to that of Eqn 5b in Buckley and Diaz-Espejo (2015). Eqn 3 can be formulated in the analogous form $\xi'(a)_{\Omega} = f\left(a_{\mathrm{m,k+1}}, \boldsymbol{b}_{\mathrm{m,k+1}}\right) - f\left(a_{\mathrm{m,k}}, \boldsymbol{b}_{\mathrm{m,k+1}}\right)$ (shown in purple in Figure 2). Because $f(a, \boldsymbol{b})$ is typically non-linear, $\xi'(\Omega)_a$ differs from $\xi(\Omega)_a$ by an error ε, see Deans et al. (2019). For instance, in Figure 2, $\xi'(a)_{\Omega}$ is 30% higher than $\xi(a)_{\Omega}$. ε decreases monotonically with *K*, therefore this issue vanishes when a suitably large value of *K* is chosen; in the examples provided *K*=1000 following Buckley and Diaz-Espejo (2015).

The key metric of contribution analysis is the 'total contribution of a to the change in Ω', which, in the transition from state I to state M, is the sum of the marginal contributions over all intermediate intervals and states:

$$\Xi(a)_{\Omega} = \sum_{m=\mathrm{I}}^{M} \sum_{k=0}^{K} \xi(a)_{\Omega} . \qquad 4$$

This definition of total contribution corresponds to that of Eqn 5c in Buckley and Diaz-Espejo (2015).

The 'relative contribution of a to the change in Ω' between the state I and the state M is:

$$\rho(a)_{\Omega} = \frac{\Xi(a)_{\Omega}}{\Omega_{\mathrm{M,K}} - \Omega_{\mathrm{I,0}}}. \qquad 5$$

The definition of relative contribution corresponds to Eqn 25 in Jones (1985).

The key metric in limitation analysis is the 'limitation by a to the change in Ω', which, between the state I and the state M is:

$$L(a)_{\Omega} = \frac{\Xi(a)_{\Omega}}{\Omega_{\mathrm{M,K}}}. \qquad 6$$

This definition of limitation corresponds to Eqn 13 in Farquhar and Sharkey (1982), Eqn 13 in Jones (1985), and to Eqn 7 in Buckley and Diaz-Espejo (2015) but expressed as percentage therein.

The key metrics in control analysis are absolute and relative sensitivity. The absolute 'sensitivity of Ω to a', calculated in a particular state and interval (m, k), is:

$$S(\Omega)_{a} = \frac{\xi(a)_{\Omega}}{a_{\mathrm{m,k+1}} - a_{\mathrm{m,k}}}. \qquad 7$$

Sensitivity, a finite-difference estimate of $\frac{\partial f}{\partial a}$, corresponds to Eqn 1 in Jones (1985) and to the partial derivatives in Eqn 1 of Buckley and Diaz-Espejo (2015).

Finally, the relative sensitivity better referred to as 'elasticity of Ω to a', calculated in a particular state (m, k), is:

$$\eta(\Omega)_{a} = \frac{\ln f(a_{\mathrm{m,k+1}}, \boldsymbol{b}_{\mathrm{m,k}}) - \ln f(a_{\mathrm{m,k}}, \boldsymbol{b}_{\mathrm{m,k}})}{\ln a_{\mathrm{m,k+1}} - \ln a_{\mathrm{m,k}}}. \qquad 8$$

Elasticity, a finite-difference estimate of $\frac{\partial Ln(f)}{\partial Ln(a)}$ correspond to the relative limitation (l_{S}, l_{M}) in Eqn 7 in Grassi and Magnani (2005), to the partial derivatives in Eqn 3 of Buckley and Diaz-Espejo (2015).

There will be as many analogous formulations of Eqns 1 to 8 as there are model inputs. All definitions given above are generally valid, but below I will only explore the case in which the output Ω is net photosynthetic CO_2 uptake (A), and the function f is hence a model of photosynthesis.

Applications

Diffusional and non-diffusional restrictions

Here I will initially use the empirical model of Prioul and Chartier (1977), because it is simple, suitable for all common restriction analyses, and can be used for C_3 and C_4 photosynthesis (Bellasio et al. 2018) as well as intermediate types alike. In the formulation of (Bellasio et al. 2016b) assimilation is:

$$A = \frac{CE\,(C - \Gamma) + A_{\mathrm{SAT}} - \sqrt{(CE[C - \Gamma] + A_{\mathrm{SAT}})^2 - (4\,\omega\,A_{\mathrm{SAT}}\,CE\,[C - \Gamma])}}{2\omega}, \qquad 9$$

where, A_{SAT} is the CO_2-saturated rate, CE is the initial slope, C may be C_{i} or C_{M}, Γ is the x-intercept, ω is defining curvature.

CO_2 enters the leaf through gaseous diffusion across stomata and the air passages between cells, dissolves in water, and diffuses in solution through the cell wall, plasmalemma and through the mesophyll to reach the Rubisco or phosphoenolpyruvate carboxylase sites of carboxylation, located in the chloroplasts of C_3 leaves or in the cytosol of C_4 leaves. The ease of this process is the total conductance $g_{\mathrm{Tot}} = \frac{g_{\mathrm{S}}\,g_{\mathrm{M}}}{g_{\mathrm{S}} + g_{\mathrm{M}}}$, where mesophyll conductance (g_{M}) compounds all processes that are not stomatal. The leaf supply function can be written as:

$$C_{\mathrm{M}} = C_{\mathrm{a}} - \frac{A}{\frac{g_{\mathrm{S}}\,g_{\mathrm{M}}}{g_{\mathrm{S}} + g_{\mathrm{M}}}}. \qquad 10$$

Combining Eqn 9 and Eqn 10 results in a quadratic for A:

$$A = \frac{CE\left(\frac{A_{\mathrm{SAT}}^2}{\frac{g_S + g_M}{g_S\,g_M}} + C_{\mathrm{a}} - \Gamma\right) - \sqrt{\left[CE\left(\Gamma - C_{\mathrm{a}} - \frac{A_{\mathrm{SAT}}^2}{\frac{g_S + g_M}{g_S\,g_M}}\right)\right]^2 - 4\left(\omega + \frac{CE}{\frac{g_S + g_M}{g_S\,g_M}}\right) A_{\mathrm{SAT}}\,CE\,(C_{\mathrm{a}} - \Gamma)}}{2\left(\omega + \frac{CE}{\frac{g_S + g_M}{g_S\,g_M}}\right)} \qquad 11$$

Eqn 11 will be used to evaluate diffusional and non-diffusional restrictions.

Stomatal limitation

Stomatal limitation is the reduction of assimilation due to stomatal closure that occurs in a leaf in a real, ordinary operational conditions as compared to a hypothetical case where CO_2 would freely enter the leaf (the maximum limit of stomatal conductance is assumed to be infinity). The fixed characteristics of the plant CE, Γ, and ω (the vector $\boldsymbol{b}$ in Eqn 1) are found by curve fitting (procedures are available in Workbook I), that is, by inputting the measured value of C_{i} in Eqn 9 and adjusting their value until Eqn 9 outputs the output value of assimilation that is most similar to that measured. The values fitted to example data are shown in Table 2. Stomatal limitation is lifted in a single transition (number 1 in Figure 1b) by calculating Eqn 11 in all K intervals between state I where g_{S} equals g_{Sop}, and state II, the hypothetical scenario where g_{S} is set to a high value (Procedures are available in Workbook II). A numerical example is shown in Figure 3A. The

corresponding calculations are shown in Sheet 1 of Workbook III, where control coefficients (Eqn 7 and 8) are calculated for each step of the transition. The same procedure can be utilized to compare two known states resulting from any environmental perturbation (transition number 3 in Figure 1b), as long as they can be described by the same A/C_i response curve, simply by entering the two relevant g_S values.

Diffusional limitation

The analysis of diffusional limitation quantifies the total effect of diffusion from atmosphere to the sites of carboxylation, and requires g_M. This not straightforward to estimate and involves combined measurements of gas exchange and variable fluorescence in C_3 plants (Bellasio et al. 2016b), or isotopic methods in C_3 and C_4 plants (Ubierna et al. 2017; Busch et al. 2020). Diffusional limitation is evaluated in the same way as stomatal limitation, using C_M in place of C_i. Practically, for each measured value of C_i, the corresponding value of C_M is calculated as $C_M = C_i - \frac{A}{g_M}$. Eqn 9 is fitted as described above, this time to the A/C_M response curve obtaining new C_M-based CE, and ω (Table 2). Eqn 11 is calculated in all K intervals between state I where g_S and g_M take the operational values and, and state II, the hypothetical scenario where g_S and g_M are high. Application is exemplified in Figure 3b and the corresponding calculations are in Sheet 2 of Workbook III.

Stomatal and non-stomatal limitation

Evaluating the stomatal limitation of treated plants using the procedure shown above (transition number 5 in Figure 1b) requires knowing the A/C_i responses of the treated plant. When these are impractical or impossible to measure, their parameters need to be estimated. In the method that I recently proposed (Bellasio 2023), the A/C_i curve of the treated plant is obtained by 'flattening' the A/C_i curve of the healthy plant (red line in Figure 2C) to match the pair ($C_{i\,op}$, A_{op}) measured for the treated plant. The assumptions made are that the curvature ω and the CO_2 compensation point Γ are not affected by the treatment, while the horizontal asymptote A_{SAT} and the initial slope CE maintain their ratio $\mu = A_{SAT}/CE$ constant. Eqn 9 is solved for CE as:

$$CE' = \frac{A\,(\mu + C - \Gamma) + \sqrt{[A\,(\Gamma - C - \mu)]^2 - \left[4\,\omega\,A^2\,\mu\,\,(C - \Gamma)\right]}}{2\mu\,(C - \Gamma)}, \qquad 12$$

CE', the estimated value of CE of the treated plant, is directly calculated by inputting measured A_{op} and C_{iop} or C_{Mop} in Eqn 12; A_{SAT}', the estimated value of A_{SAT} in the treated plant, is, by assumption, $\mu\,CE'$. The difference between the potential attained by the treated plant and that of the healthy plant is conventionally referred to as non-stomatal limitation, which can be evaluated in a second transition (number 6 in Figure 1b). The procedure is shown in Figure 3C and the corresponding calculations and control analyses are shown for each step in Sheet 3 of workbook III.

An alternative procedure, proposed here anew, lifts limitations in a single transition between the operational conditions of the treated plant and the potential conditions of the healthy plant (number 7 in Figure 1b).

If A/C_i curves and g_M are available for both the healthy and the treated plants, diffusional limitation can be resolved in its mesophyll and stomatal components. A first transition may lift diffusional limitation (number 8 in Figure 1b), while a second transition may lift non-diffusional limitation, as for non-stomatal limitation (number 6 in Figure 1b). A single transition lifting diffusional and non-diffusional limitation concurrently is also possible. Also these two alternatives are new to this study.

Stomatal, mesophyll and non-diffusional contributions

If A/C_i curves and g_M are available for both the healthy and the treated plants, the effect of the treatment can be resolved in its biochemical, mesophyll and stomatal components in a single transition (number 4 in Figure 1b). This is essentially a simple generalisation of the method of Buckley and Diaz-Espejo (2015). A numerical example is shown in Figure 3D, and the corresponding calculations and control analysis are in Sheet 4 of Workbook III. If g_M for the treated plant is not available, the corresponding transition (number 3 in Figure 1b) can be implemented in with the same procedure, using the C_i-based parameterisation, and by setting an arbitrarily high value for g_M. This variant is new to this study.

Control analysis

The extent to which assimilation is controlled by a marginal change in the underpinning variables (typically, g_S and g_M alongside other inputs in $\boldsymbol{b}$) is quantified by sensitivity. The strength of this analysis lies in being univocal in any given state, allowing for independent evaluation of plants (*e.g.* healthy plants under ordinary operational conditions) and *a posteriori* comparison (*e.g.* across species in the phylogeny (Gago et al. 2019)).

This analysis can be implemented using the logic of previous examples by imagining that the transition between states becomes arbitrarily small. In practice, Eqn 11 is used calculated for the state of interest, and that in which g_S and g_M (alongside A_{SAT}, CE, ω, and Γ, or a subset thereof) differ by a marginal increment ($i = \frac{da}{a} = dLna$, for $i \rightarrow 0$). Calculations for the healthy plant (Table 2) with i=0.0001 applied to g_S, g_M, A_{SAT}, and CE are included in Sheet 7 of Workbook III. The key outputs are absolute and relative sensitivity (for instance, $S(A)_{g_S}$ averaged 113 μmol mol^{-1}, $\eta(A)_{g_S}$ averaged 0.5), and the relative change in assimilation, which adds to unity when compounding all inputs (in the example, $\rho(A)_{g_S}$ was 0.5 $\rho(A)_{g_M}$ was 0.09, $\rho(A)_{A_{SAT}}$ was 0.17, and $\rho(A)_{CE}$ was 0.25). In small transitions, $\eta(A)_{g_S}$ and $\eta(A)_{g_M}$ correspond to l_S and l_M calculated after Grassi and Magnani (2005) while $L(g_S)$ and $L(g_M)$ correspond to S_L and MC_L in their Eqn 6.

Light and non-light restrictions

Light limitation

Light limitation analysis can be utilized to quantify the reduction of assimilation due to shading, relative to a hypothetical case where the leaf would be exposed to maximum lighting. Similar to the procedure used for stomatal limitation analysis, light response curves are measured under specific growth conditions (CO_2 concentration, temperature, *etc.*). Then, the dependence of assimilation on light intensity is described with the model of Prioul and Chartier (1977) after Bellasio et al. (2016b) as:

$$GA_{MOD} = \frac{Y(CO_2)_{\mathrm{LL}}\, PPFD + GA_{\mathrm{SAT}} - \sqrt{(Y(CO_2)_{\mathrm{LL}}\, PPFD + GA_{\mathrm{SAT}})^2 - 4\, m\, Y(CO_2)_{\mathrm{LL}}\, PPFD\, GA_{\mathrm{SAT}}}}{2\, m} \qquad 13$$

Eqn 13 (coded in the 'GAvPPFD' Sheet of Workbook I) is fitted to the experimental data to derive the parameters for the healthy plant. Light limitation is quantified by evaluating a single transition between operational conditions, and where light limitation is assumed to be absent (number 1 in Figure 1c), using the procedures described in Workbook II. A worked example is provided in Sheet 6 of Workbook III.

Light contribution

The previous procedure is apt for analysing light contributions between two real conditions of interest by specifying the second condition in the parameterization of State II (number 2 in Figure 1c).

Light and non-light limitations

The analysis of light and non-light limitations can be used to distinguish the effect on assimilation directly due to shading from that due to the downregulation of the biochemical potential that occurred in a treated plant. Analogous to the approach used to resolve diffusional and non-diffusional limitations, two variants are possible. In the first case, light limitation is lifted first (number 3 in Figure 1c), and the remainder is the difference with the potential of the healthy plant (number 4 in Figure 1c). Alternatively, limitations are lifted in a single transition (number 5 in Figure 1c, exemplified in Sheet 7 of Workbook III).

Mechanistic models

The empirical models shown above are suitable for most applications, including when parameters of mechanistic models are available from previous experiments. Empirical parameters can be estimated approximately: CE corresponds to $\frac{V_{\mathrm{MAX}}}{K}$ (where V_{MAX} may be Rubisco or PEP carboxylase maximum rates and K is the corresponding Michaelis-Menten constant, adjusted for oxygen concentration in Rubisco's case); $A_{\mathrm{SAT}} \approx \frac{J}{4} - R_{\mathrm{L}}$, where J is the rate of electron transport, and R_{L} is light respiration, or, for C_4 plants $A_{\mathrm{SAT}} \approx \frac{J_{\mathrm{ATP}}}{5.5} - R_{\mathrm{L}}$, where J_{ATP} is the rate of ATP production; Γ is typically available in the literature (alternatively, it can be calculated from R_{L} and K using, for instance, Eqn 2.38 or Eqn 4.50 in von Caemmerer (2000) for C_3 plants or C_4 plants, respectively); whilst the curvature ω can typically be assumed as 0.7. For a more precise analysis, it is recommended to generate synthetic A/C response curves using 10-15 values of C_{i} (or C_{M}) as inputs for the same mechanistic model formulations from which the mechanistic parameters were originally derived. These synthetic A/C curves can then be used to derive empirical parameters through curve fitting, and then used to evaluate restrictions, as described above.

Specific applications may require direct use of mechanistic models in restriction analyses. Mechanistic models are typically more complicated than empirical, rely on a number of assumptions, are valid only when assumptions hold (*e.g.* a C_4 model is not meaningful for mechanistically describing C_3 plants) and they are less flexible in data fitting. In general, they are recommended only for cases where a description of the processes is specifically required. For instance, they can resolve non-diffusional restrictions, such as distinguishing between those due to light reactions or carbon metabolism. Well-thought-out procedures are needed, designed specifically to address the experimental question.

The method presented by Buckley and Diaz-Espejo (2015) differs from the analysis of mesophyll, stomatal, and non-diffusional contributions exemplified above only in that it uses an update of the C_3 model by Farquhar et al. (1980). This model has previously been used for the analysis of limitations imposed by Rubisco activation in its enzyme limited submodel (Deans et al. 2019) or in the full formulation (Taylor and Long 2017), and can also be used to quantify limitations imposed by electron transport and triose phosphate utilisation (Buckley and Diaz-Espejo 2015). However, this method is less widely applicable than the empirical procedure described above: it is meaningful only for C_3 plants; obtaining specific values for the Rubisco Michaelis-Menten constants for carboxylation and oxygenation (K_{C} and K_{O}) for measured leaves may not be readily achievable, and the cut-off point for enzyme and light limitation must be assumed.

A C_4 mechanistic model may serve for the quantification of restrictions due to diffusion through stomata or the mesophyll, as well as restrictions caused by other factors like light intensity, the light-saturated rate of ATP generation (J_{SAT}), the curvature of the light dependence of ATP

generation (θ), the initial quantum yield for ATP generation $Y(J_{ATP})_{LL}$, respiration in the light, Rubisco and phosphoenolpyruvate carboxylase CO_2 saturated rate of carboxylation (V_{CMAX} and V_{PMAX}), the factor that partitions ATP between PEP regeneration and the remainder of photosynthetic activity (x), and bundle sheath conductance (g_{BS}). For example, it can be used to determine the contribution of light versus that of g_{BS} in the reduction of assimilation for plants grown under shading (Bellasio and Griffiths 2014b). For a corrected formulation refer to Bellasio et al. (2017).

For simulating more complex scenarios and addressing a broad range of questions relating carbon and light reactions I recommend utilizing the Bellasio and Farquhar (2019) and Bellasio and Ermakova (2022) analytical models. The analytical model of Bellasio and Farquhar (2019) allows the quantification of limitations imposed by a wide range of real or imagined scenarios, in any photosynthetic type (C_3, C_2, C_2+C_4, C_4), intermediates thereof, and engineered transitions between them, stomatal opening and closure, different stomatal responsiveness to biochemical forcing or drought, and a wide range of characteristics of the electron transport chain (*e.g.* shifting the ratio between ATP and NADPH production by modifying the fraction of cyclic electron flow or the NDH pathway, *etc.*). The analytical model of C_4 photosynthesis of Bellasio and Ermakova (2022) relates to leaf anatomy following Bellasio and Lundgren (2016) and explicitly accounts for light harvesting partitioning between cell compartments. It was specifically developed for studying differences between C_4 photosynthetic subtypes, and maintains validity at very low irradiance. It features two electron transport chains, C_4 cycle reactions, and C_3 cycle reactions accommodating a variety of possibilities for parameterisation.

Discussion

I set out to generalise the analyses of photosynthetic restrictions, providing a set of definitions that integrate all common and several new procedures, which I illustrated using synthetic data.

The new framework is general, as it is valid for all photosynthetic types and models, and it comprehensively quantifies limitations, contributions, and photosynthetic control (sensitivity and elasticity) within a single procedure. This represents a significant advancement since the most widely used protocols – control analysis (Grassi and Magnani 2005), contribution analysis (Buckley and Diaz-Espejo 2015) and limitation analysis (Farquhar and Sharkey 1982) – were traditionally independent. This method is formulated using the principles of Buckley and Diaz-Espejo (2015), and I demonstrated its convergence with Farquhar and Sharkey (1982) and Grassi and Magnani (2005) for small transitions (see 'Control analysis' section). For complete generalisation, I also formulated within this framework the method of Björkman et al. (1980), which, although widely used, has never been formalised (Figure S1a, and discussed below).

When only one quantity varies, procedures are unambiguous. This is the case for diffusional limitation and light limitation analyses, which are evaluated by formulating calculations so that only

one quantity (variable *a* in Eqn 1) varies between transitions, while the other inputs (vector ***b*** in Eqn 1) remain constant. In all those cases the method is equivalent both for limitation and contribution analysis. When multiple quantities vary, methodological variants are possible (the number of variables changing raised to the power of the number of transitions), but choices are straightforward or alternatives are interchangeable, as I will now discuss.

In contribution analysis, all quantities can be presumed to change concurrently and linearly between their initial and final values (number 3 in Figure 1b), as proposed by Buckley and Diaz-Espejo (2015), thus there is no longer ambiguity in the path to follow. In classical literature, it had been proposed to assume that stomata respond before any change in leaf biochemical processes occurs, or the reverse. The discrepancy between paths was often large, for instance Assmann (1988) reported a five-fold difference. I calculated both path dependent alternative (shown in Figure S1b and calculated in sheets 9 and 10 of Workbook III), and found that the discrepancy for stomatal contribution was relatively small about ±20% of the independent path. Yet, path dependent methods are not recommended. While their assumptions may partially hold under specific conditions, such as when stomatal adjustment is much slower than photosynthetic activation (Deans et al. 2019), they are generally invalid. In fact, during the imposition of a treatment, photosynthetic characteristics typically respond progressively, driven by a common factor – the treatment – and are therefore not independent.

In the analysis of limitations, there is the possibility to opt for a single or two-tiered transition. The distinction is merely conceptual, as the results do not differ. Much of the past debate has been driven by methodological papers prioritizing the breadth of alternative approaches rather than narrowing their choice. In contrast, focusing on the experiment and its research questions will naturally determine the appropriate method to follow. Plants are often subject to permanent or mid-term acclimation treatments (*e.g.*, differing nitrogen levels, watering levels, growth light conditions, growth CO_2 levels, soil types, fertilisation, mycorrhization, *etc.*), or differ by any genetic trait, whether natural or engineered. These traits are not subject to short-term changes, and it is possible to devise a hypothetical scenario whereby limitations are lifted independently, assuming the characteristics of the plant remain constant. Applying this principle involves evaluating two transitions (numbers 5 and 6 in Figure 1b), which is the conventional approach used in the literature. I presented a novel single-transition variant for limitation analysis (number 7 in Figure 1b), which has the benefit of being univocally defined. Under current assumptions – that inputs scale linearly (Eqn 2) and diffusional limitations are fully lifted in the idealized state, where the total conductance to CO_2 becomes high – the single-transition variant accurately tracks the two-transition variant, without differences in results. (This can be verified by typing 1 in cell C1 and "n" in cell F10 in Sheet 3 of Workbook III) Therefore, unless additional assumptions are introduced, they can be used interchangeably.

Sometimes it may be difficult to determine the characteristics ***b*** of the treated plants. Through an elegant experimental routine, Taylor and Long (2017) measured rapid A/C_i responses in real time during the treatment's course, using modern gas exchange equipment and routines (Stinziano et al. 2017). However, often this is impractical; in which case the characteristics of treated plants must be estimated. A simple and widely used method is that of Björkman et al. (1980), which the estimation follows the assumption that lifting stomatal limitation in the treated plant would result in the same increase in assimilation as in the healthy plant (details and mathematical formalisation in Figure S1a). This simplification is generally acceptable for C_4 plants because their A/C_i curves are flat for $C_i > C_{iop}$. For C_3 plants, it may be acceptable only when the treatment effect is small, but stomatal limitation is overestimated when the assimilatory potential is severely reduced by the treatment. The method I followed here to derive an analytical solution is based on Bellasio (2023). It involves flattening the A/C_i curves of treated plants, under the assumption that CE and A_{SAT} maintain their ratio (Eqn 12). This corresponds mechanistically to fixing the J/V_{MAX} ratio, and may not have general validity, as the treatment's effect on parameters may be species- and treatment-dependent. The coded procedure allows to input the actual ratio, which should be preferred if available. Γ and ω are maintained invariant based on the rationale that they are underpinned by enzymatic properties (see 'Mechanistic models' above), and indeed measurements show that, for instance, they did not significantly change in both C_3 and C_4 plants during seasonal drought (Bellasio et al. 2022).

The framework avoids two erroneous practices: that of approximating curves with lines in finite intervals (see Introduction), and that of overestimating their slopes. The latter practice was introduced by Tomás et al. (2013) and gained traction in later studies, for instance by Tosens et al. (2016); Carriquí et al. (2015); Carriquí et al. (2019); Perera-Castro et al. (2022); Hu et al. (2024). The slope of the A/C_M response curves required for the linear approximation of the infinitesimal analysis of Grassi and Magnani (2005) was derived under low CO_2 concentrations – where it is typically several-fold higher than under ordinary operational conditions. This inevitably leads to largely overestimating the importance of stomata and mesophyll diffusion – and has likely brought to overstating their importance – in restricting assimilation.

The analysis of light and non-light restrictions is original to this study. Lifting light limitation may not involve exposing leaves to infinite light intensity but just to full sunlight, making it difficult to pinpoint the real versus hypothetical conditions, creating confusion between contribution and limitation analyses. A decrease in assimilation may result from a combination of direct and indirect effects of shading, such has the decrease in biochemical potential that occurs in a leaf shaded by the overgrowth of a new canopy (Bellasio and Griffiths 2014a). Because these responses are not independent, in this case the analysis of contributions in a single transition may be appropriate. Alternatively, if the treatment has affected the biochemical potential independently of light, such as in cases of pathogen attack or nitrogen level changes (Dewar et al. 2012), then limitation analysis with a two-tiered transition may be preferable.

Conclusion

I urge the community to critically reconsider the relative importance of stomatal, mesophyll, and non-diffusional restrictions, especially when they were evaluated using the linear approximation in finite intervals by Grassi and Magnani (2005), and the initial slopes of the A/C_M curves by Tomás et al. (2013), which are erroneous.

Availability

The workbooks coding curve fitting, procedures for restriction analysis and worked examples are available in the Supporting Information of this article. A curated version is available on GitHub at the link [https://github.com/chandrabellasio/Quantifying-Photosynthetic-Restrictions-]. The C_3 and C_4 models of Farquhar et al. (1980) and Berry and Farquhar (1978) in the formulations of Bellasio et al. (2017) can be made available upon request. Spreadsheets coding the Bellasio and Farquhar (2019) and Bellasio and Ermakova (2022) analytical models are available in the Supporting Information of the original publications.

Acknowledgments

This work slowly emerged from the requests I received during the four years of the gestation of my previous commentary (Bellasio 2023), eventually expanding into a standalone paper. Reaching this point would have been impossible without the trust of Editor Patrick Morgan and the patience of the reviewers, who managed to navigate my early drafts and provide the suggestions that shaped this research at various stages. I am grateful to Alessio Fini, Hilary Stuart-Williams, Ross Deans, and Jaume Flexas for their valuable discussions.

I have no competing interests.

Funding

I gratefully acknowledge funding by a Science Foundation Ireland Individual Pathway Fellowship (21/PATH-S/9322), and by a European Union's Horizon 2020 research and innovation programme MSCA individual fellowship (grant agreement ID No: 702755).

450

Table 1. Acronyms, definitions, variables, and units used

Symbol	Definition	Units
a	any generic input of a mathematical model	
A, A_{op}	Net assimilation, unspecified or measured under ordinary, operational conditions	µmol CO_2 m^{-2} s^{-1}
A_{SAT}, A_{SAT}'	CO_2 saturated *A*, unspecified of after a generic treatment, respectively	µmol $CO_2 m^{-2}$ s^{-1}
b	a generic set of inputs of a mathematical model which includes all parameters and variables that are not *a*	
C_a	CO_2 concentration outside the leaf	µmol CO_2 mol air^{-1}
CE, CE'	Initial slope of the A/C_i curve, unspecified of after a generic treatment, respectively	mol air m^{-2} s^{-1}
C_i, C_{iop}	CO_2 concentration in the substomatal cavity as calculated by the IRGA, unspecified, or under operational conditions	µmol CO_2 mol air $^{-1}$
C_M	CO_2 concentration at the mesophyll carboxylating sites	µmol CO_2 mol air $^{-1}$
Contribution	Any change in an output variable which is due to a change only in one input, it can be marginal [small csi, ξ, Eqn 3], total [capital csi, Ξ, Eqn 4], or relative [eta, η, Eqn 5].	µmol m^{-2} s^{-1}, the relative is dimensionless
E	Leaf level water transpiration rate	mmol H_2O m^{-2} s^{-1}
g_{BS}	Bundle sheath conductance to CO_2 diffusion	mol m^{-2} s^{-1}
g_M	Mesophyll conductance to CO_2 diffusion	mol air m^{-2} s^{-1}
g_S	Stomatal conductance, here to CO_2 diffusion also when unspecified, elsewhere often referred to as g_{SC}	mol air m^{-2} s^{-1}
g_{Tot}	Total conductance to CO_2 diffusion, the reciprocal of g_{Tot} is the sum of the reciprocal of g_S plus the reciprocal of g_M	µmol m^{-2} s^{-1}
k, K	Any generic interval between states and the total number of intervals, respectively	
Limitation	The total contribution divided by the maximum value of the function in the interval, Eqn 6	
L_{NS}	Non-stomatal limitation to photosynthesis	dimensionless
L_S	Stomatal limitation to photosynthesis	dimensionless
m, M	Any generic state, and the total number of states, respectively	
Restriction	Any generic hindrance to photosynthetic activity	
Sensitivity	The marginal contribution divided by the value of the variable, relative to the change in input divided by the value of the input, Eqn 7	
State	Any condition in which a photosynthetic model can be defined (by knowing *a* and ***b***)	
µ	A_{SAT} divided by *CE*	
Ω	Any generic output of a mathematical model, a function of *a* and ***b***	
ω	Curvature of the non-rectangular hyperbola describing the C_i dependence of *A*	dimensionless

451

Table 2. Synthetic data used in the examples

Plants were either untreated or subjected to a hypothetical treatment which reduced the photosynthetic potential. The rates of assimilation (A) and CO_2 concentration in the substomatal cavity (C_i) attained in the conditions in which plants were grown are denoted as operational. Gas exchange measurements at the lab bench determined the responses of A to C_i. Values of CO_2 concentration at the sites of carboxylation was calculated using mesophyll conductance values of 0.35 mol m^{-2} s^{-1} and 0.25 mol m^{-2} s^{-1}, previously obtained for healthy plants and treated plants, respectively. Assimilation is expressed in µmol m^{-2} s^{-1}, CO_2 concentration in µmol mol^{-1}. Non-rectangular hyperbolas were fitted either to the A/C_i or to A/C_M curves to obtain two sets of fitted parameters reported at the bottom using the fitting tool of Bellasio et al. (2016b), copied in the sheet 'AvCi' of the workbook provided in Supporting Information for convenience.

Measured	**Healthy**			**Treated**		
Operational	A_{op}	$C_{i\ op}$	$C_{M\ op}$	A_{op}	$C_{i\ op}$	$C_{M\ op}$
	13.9	200	160	11	220	176
A/C Response	A	C_i	C_M	A	C_i	C_M
	-2.59	24	32	-1.91	24	32
	-1.22	35	38	-0.90	35	39
	0.60	50	48	0.44	50	48
	3.00	71	62	2.21	71	62
	6.15	101	84	4.53	101	83
	10.1	145	116	7.42	145	115
	14.4	210	166	10.6	210	164
	17.9	294	243	13.2	294	242
	20.7	420	361	15.2	420	359
Fitted		**C_i-based**	**C_M-based**		**C_i-based**	**C_M-based**
A_{SAT} / µmol m^{-2} s^{-1}		26	26		19	19
CE / mol m^{-2} s^{-1}		0.12	0.18		0.09	0.14
ω		0.7	0.54		0.7	0.54
Γ / µmol mol^{-1}		45	45		45	45

Figure 1. Generalised framework of restriction analysis

Restrictions may be evaluated along a real and an hypothetical dimensions. The analysis of limitations quantifies the restriction independently in each plant, compared their maximum potential. The analysis of contribution analyses the transition between two real conditions. The analysis of control (sensitivity and elasticity) can be done at any intermediate points of the transitions (exemplified by a 'C' in a green circle that may be swinging over all arrows). Panel (a) general framework; Panel (b) diffusional and non-diffusional restrictions; Panel (c) light and non-light restrictions.

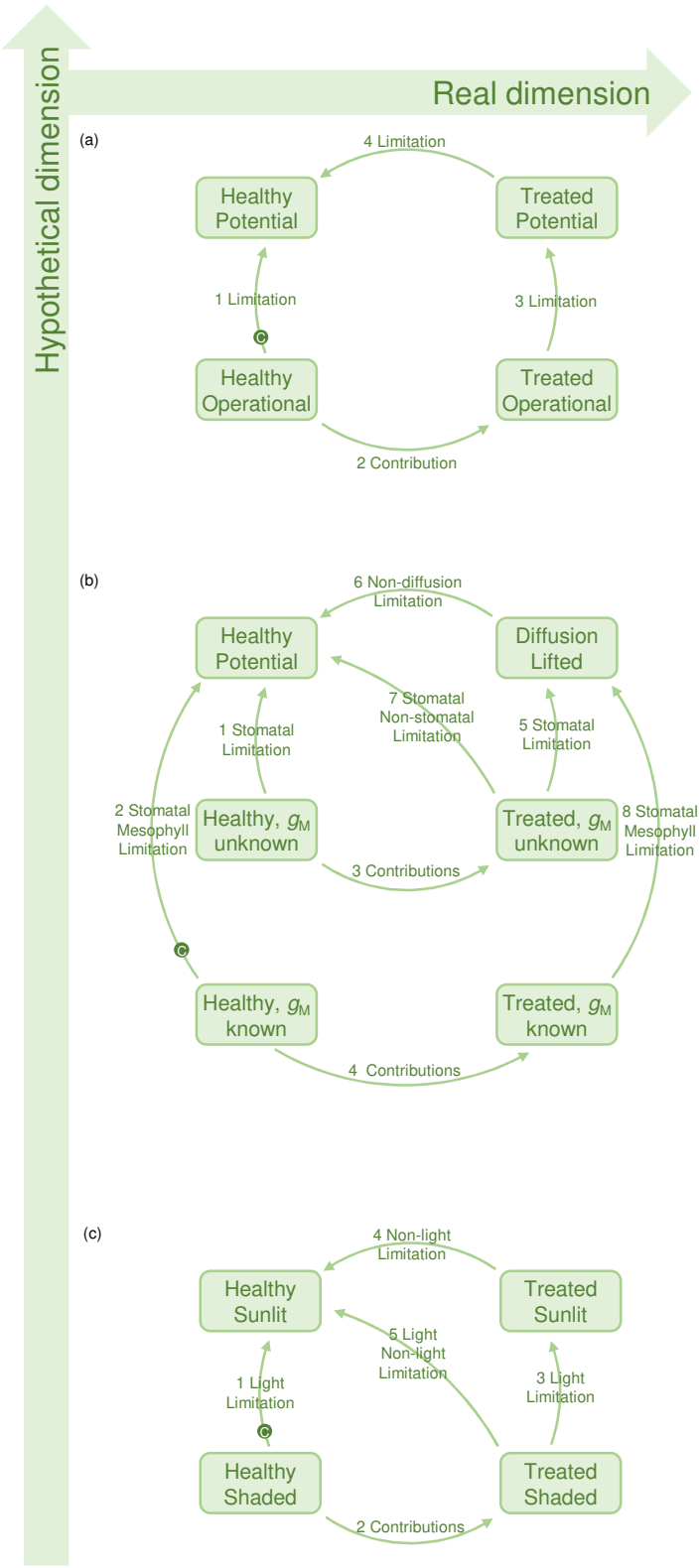

Figure 2. Schematic of the generalised framework of definitions

A generic output variable Ω is described through a mathematical model as a function of the variable a (in abscissa) and a set of other inputs $\boldsymbol{b}$. The conditions in which a and **b** are known are called 'states', here represented by two black diamonds. The function $\Omega = f(a, \boldsymbol{b})$ parameterised with the known vector $\boldsymbol{b}$, for state I is shown in red, and for state II is shown in blue. The transition between the two known states is divided in four equal intervals, which are bordered by thin black lines. The value of the inputs a and $\boldsymbol{b}$ is assumed to vary linearly in the intervals. The marginal contribution ξ of the variable a to the change in the output Ω is shown in purple. The value of ξ' becomes equal to that of ξ for large values of K.

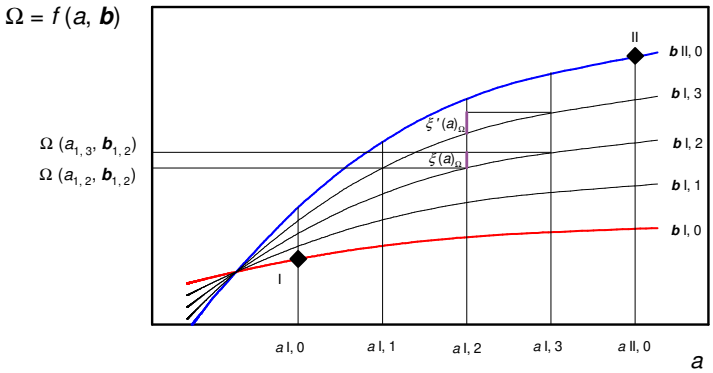

Figure 3. Quantifying limitations and contributions to changes in photosynthesis

Stomatal limitation. Panel **A** shows a photosynthetic model describing the dependence of assimilation (A) upon CO_2 concentration in the substomatal cavity (C_i, solid line, Eqn 9) of healthy plants (blue). In this example with hypothetical data, operational conditions correspond to an ambient CO_2 concentration (C_a) of 420 µmol mol^{-1} and a fixed light intensity (the level is irrelevant here). It attains a rate of assimilation (A_{op}) of 13.9 µmol m^{-2} s^{-1}, and has a CO_2 concentration in the substomatal cavity ($C_{i\,op}$) of 200 µmol mol^{-1}, corresponding to an operational stomatal conductance to CO_2 $\left[g_{SC\,op} = \frac{A_{op}}{C_a - C_{i\,op}}\right]$ of 0.063 mol m^{-2} s^{-1} (Table 2). In the transition between operational State I and hypothetical State II assimilation is driven to its potential as if intercellular spaces were directly exposed to external CO_2 concentration, C_a (Eqn 9 calculated for $C_i = C_a$). Assimilation increased from 13.9 to 20.7 µmol m^{-2} s^{-1}; the total contribution of C_i to the change in assimilation $[\Xi(C_i)_A]$ was 6.9 µmol m^{-2} s^{-1}; the relative contribution of C_i to the change in assimilation $[\rho(C_i)_A]$ was 1 because C_i was the only input to vary between the two states; the limitation imposed by C_i to assimilation $[L(C_i)_A]$ corresponds to stomatal limitation, was 0.33. $S(\Omega)_a$, and $\eta(\Omega)_a$ are shown in Sheet 1 of Workbook III, calculated for each step of the transition.

Diffusional limitation. Panel **B** shows the modelled dependence of assimilation (A) upon CO_2 concentration in the mesophyll (C_M, dashed line, Eqn 9) of healthy plants. Diffusional limitation is quantified by evaluating transitions from the operational conditions of state I with physiological g_M and g_S, to a state II where the hindrance to CO_2 diffusion caused both by the stomata and by the mesophyll is removed by increasing g_M and g_S to high values. Assimilation increased from 13.9 in state I, to 21.5 µmol m^{-2} s^{-1} in state II; diffusional limitation was 0.36; details are in Sheet 2 of workbook III.

Stomatal and non-stomatal limitation. Panel **C** shows the modelled A/C_i curves of healthy (blue) and treated (red) plants. State I is the operational conditions of the treated plant (diamond 'I'). State II is where, with otherwise invariant parameterisation, the stomatal barrier is removed by increasing g_M and g_S so that C_i reaches approximately the value of C_a of 420 µmol mol^{-1}. State III is where C_a is invariant, while the parameters A_{SAT} and CE are driven to those of the reference plant. The treated plant had an A_{op} of 11 µmol m^{-2} s^{-1}, and a $C_{i\ op}$ of 220 µmol mol^{-1}, the healthy plant is the same (Table 2). In the transitions, assimilation increased from A_{op} of 11 in state I, to A_{Ca} of 15.2 µmol m^{-2} s^{-1}in state II to A_{Pot} of 20.7 µmol m^{-2} s^{-1} in state III. Stomatal limitation, $L(g_S)_A$, was 0.20; the sum of the other limitations (A_{SAT}, CE, ω, and Γ), that is, non-stomatal limitation, was 0.26. Calculations are shown in Sheet 3 of Workbook III.

Contribution analysis. Panel **D** shows the modelled A/C_M curves of healthy (blue) and treated plants (red). Healthy plants' A/C_M responses, A_{op}, $C_{M\ op}$, $g_{SC\ op}$ and g_M are from previous examples while $g_{SC\ op}'$ was 0.055 mol m^{-2} s^{-1}. Parameters of the fitted to A/C_M responses are in Table 2. State I and II represent generic operational points of healthy and treated plants, respectively. Stomatal, mesophyll and non-diffusional contribution are quantified in a single transition whereby quantities change linearly between values of healthy and treated plants. The total diffusional contribution was -0.9 µmol m^{-2} s^{-1}, resolved in a stomatal contribution of -0.5 µmol m^{-2} s^{-1}, and a mesophyll contribution of -0.4 µmol m^{-2} s^{-1}. The total non-diffusional contribution was -1.7 µmol m^{-2} s^{-1}. The calculations are in Sheet 4 of Workbook III.

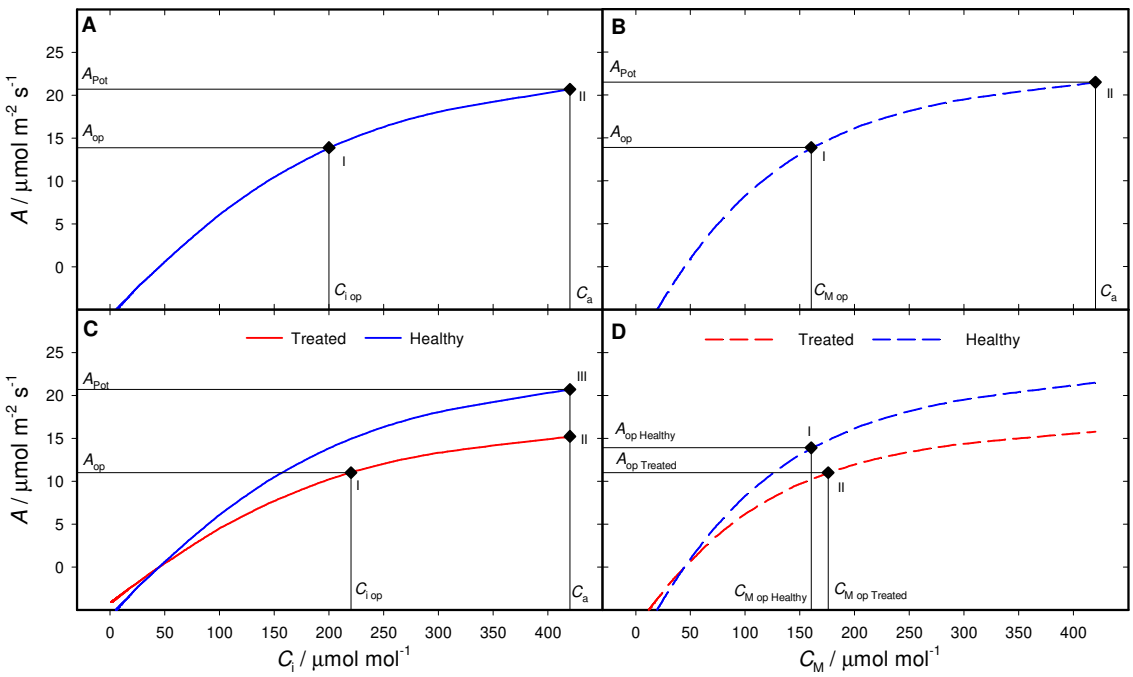

References

Assmann S (1988) Stomatal and non‐stomatal limitations to carbon assimilation: an evaluation of the path‐dependent method. Plant, Cell & Environment 11 (7):577-582.

Bellasio C (2023) The slope of assimilation rate against stomatal conductance should not be used as a measure of water-use efficiency or stomatal control over assimilation. Photosynth Res 158:195-199.

Bellasio C, Beerling DJ, Griffiths H (2016a) Deriving C_4 photosynthetic parameters from combined gas exchange and chlorophyll fluorescence using an Excel tool: theory and practice. Plant, Cell & Environment 39 (6):1164-1179.

Bellasio C, Beerling DJ, Griffiths H (2016b) An Excel tool for deriving key photosynthetic parameters from combined gas exchange and chlorophyll fluorescence: theory and practice. Plant Cell Environ 39 (6):1180–1197.

Bellasio C, Ermakova M (2022) Reduction of bundle sheath size boosts cyclic electron flow in C4 Setaria viridis acclimated to low light. The Plant Journal 111 (5):1223-1237.

Bellasio C, Farquhar GD (2019) A leaf-level biochemical model simulating the introduction of C2 and C4 photosynthesis in C3 rice: gains, losses and metabolite fluxes. New Phytologist 223 (1):150-166.

Bellasio C, Griffiths H (2014a) Acclimation of C4 metabolism to low light in mature maize leaves could limit energetic losses during progressive shading in a crop canopy. Journal of Experimental Botany 65 (13):3725-3736.

Bellasio C, Griffiths H (2014b) Acclimation to Low Light by C4 maize: Implications for Bundle Sheath Leakiness. Plant Cell Environ 37 (5):1046-1058.

Bellasio C, Lundgren MR (2016) Anatomical constraints to C4 evolution: light harvesting capacity in the bundle sheath. New Phytologist 212 (2):485–496.

Bellasio C, Quirk J, Beerling DJ (2018) Stomatal and non-stomatal limitations in savanna trees and C4 grasses grown at low, ambient and high atmospheric CO2. Plant Science 274:181-192.

Bellasio C, Quirk J, Buckley TN, Beerling D (2017) A dynamic hydro-mechanical and biochemical model of stomatal conductance for C4 photosynthesis. Plant Physiol 175 (1):104-119.

Bellasio C, Quirk J, Ubierna N, Beerling DJ (2022) Physiological responses to low CO2 over prolonged drought as primers for forest-grassland transitions. Nature Plants 8:1014–1023.

Bellasio C, Stuart-Williams H, Farquhar GD, Flexas J (2023) C4 maize and sorghum are more sensitive to rapid dehydration than C3 wheat and sunflower. New Phytologist 240 (6):2239-2252.

Berry JA, Farquhar GD (1978) The CO2 concentrating function of C4 photosynthesis: a biochemical model. In: Hall D, Coombs J, Goodwin T (eds) Proceedings of the 4th International Congress on Photosynthesis, Reading, 1978. Biochemical Society, London, pp 119-131

Björkman O, Downton WJS, Mooney HA (1980) Response and adaptation to water stress in Nerium oleander. Carnegie Institute Washington Yearbook 79:150–157.

Buckley TN, Diaz-Espejo A (2015) Partitioning changes in photosynthetic rate into contributions from different variables. Plant, Cell & Environment 38 (6):1200-1211.

Busch FA, Ainsworth EA, Amtmann A, Cavanagh AP, Driever SM, Ferguson JN, Kromdijk J, Lawson T, Leakey ADB, Matthews JSA, Meacham-Hensold K, Vath RL, Vialet-Chabrand S, Walker BJ, Papanatsiou M (2024) A guide to photosynthetic gas exchange measurements: Fundamental principles, best practice and potential pitfalls. Plant, Cell & Environment https://doi.org/10.1111/pce.14815 (n/a).

Busch FA, Holloway-Phillips M, Stuart-Williams H, Farquhar GD (2020) Revisiting carbon isotope discrimination in C3 plants shows respiration rules when photosynthesis is low. Nature Plants 6 (3):245-258.

Cano FJ, Sharwood RE, Cousins AB, Ghannoum O (2019) The role of leaf width and conductances to CO2 in determining water use efficiency in C4 grasses. New Phytologist 223 (3):1280-1295.

Carriquí M, Cabrera HM, Conesa MÀ, Coopman RE, Douthe C, Gago J, GallÉ A, GalmÉS J, Ribas-Carbo M, TomÁS M, Flexas J (2015) Diffusional limitations explain the lower photosynthetic capacity of ferns as compared with angiosperms in a common garden study. Plant, Cell & Environment 38 (3):448-460.

Carriquí M, Roig‐Oliver M, Brodribb TJ, Coopman R, Gill W, Mark K, Niinemets Ü, Perera‐Castro AV, Ribas‐Carbó M, Sack L (2019) Anatomical constraints to nonstomatal diffusion conductance and photosynthesis in lycophytes and bryophytes. New Phytologist 222 (3):1256-1270.

Deans RM, Farquhar GD, Busch FA (2019) Estimating stomatal and biochemical limitations during photosynthetic induction. Plant, Cell & Environment 42 (12):3227-3240.

Dewar RC, Tarvainen L, Parker K, Wallin G, McMurtrie RE (2012) Why does leaf nitrogen decline within tree canopies less rapidly than light? An explanation from optimization subject to a lower bound on leaf mass per area. Tree Physiology 32 (5):520-534.

Farquhar GD, Sharkey TD (1982) Stomatal Conductance and Photosynthesis. Annual Review of Plant Physiology and Plant Molecular Biology 33:317-345.

Farquhar GD, von Caemmerer S, Berry JA (1980) A biochemical-model of photosynthetic CO2 assimilation in leaves of C3 species. Planta 149 (1):78-90.

Gaastra P (1959) Photosynthesis of crop plants as influenced by light, carbon dioxide, temperature, and stomatal diffusion resistance. Veenman,

Gago J, Carriquí M, Nadal M, Clemente-Moreno MJ, Coopman RE, Fernie AR, Flexas J (2019) Photosynthesis optimized across land plant phylogeny. Trends in Plant Science 24 (10):947-958.

Grassi G, Magnani F (2005) Stomatal, mesophyll conductance and biochemical limitations to photosynthesis as affected by drought and leaf ontogeny in ash and oak trees. Plant, Cell & Environment 28 (7):834-849.

Hu W, Loka DA, Yang Y, Wu Z, Wang J, Liu L, Wang S, Zhou Z (2024) Partial root-zone drying irrigation improves intrinsic water-use efficiency and maintains high photosynthesis by uncoupling stomatal and mesophyll conductance in cotton leaves. Plant, Cell & Environment DOI: 10.1111/pce.14932 (n/a).

Jarvis P (1971) The estimation of resistances to carbon dioxide transfer. Plant photosynthetic production Manual of methods.

Jones H (1985) Partitioning stomatal and non‐stomatal limitations to photosynthesis. Plant, Cell & Environment 8 (2):95-104.

Jones H, Slatyer R (1972) Estimation of the transport and carboxylation components of the intracellular limitation to leaf photosynthesis. Plant Physiol 50 (2):283-288.

Jones HG (1973) Limiting factors in photosynthesis. New Phytologist 72 (5):1089-1094.

Perera-Castro AV, Waterman MJ, Robinson SA, Flexas J (2022) Limitations to photosynthesis in bryophytes: certainties and uncertainties regarding methodology. Journal of Experimental Botany 73 (13):4592-4604.

Prioul J, Cornic G, Jones H Discussion of stomatal and non stomatal components in leaf photosynthesis decline under stress conditions. In: Advances in Photosynthesis Research: Proceedings of the VIth International Congress on Photosynthesis, Brussels, Belgium, August 1–6, 1983. Volume 4, 1984. Springer, pp 375-378

Prioul JL, Chartier P (1977) Partitioning of Transfer and Carboxylation Components of Intracellular Resistance to Photosynthetic CO2 Fixation: A Critical Analysis of the Methods Used. Ann Bot-London 41 (4):789-800.

Stinziano JR, Morgan PB, Lynch DJ, Saathoff AJ, McDermitt DK, Hanson DT (2017) The rapid A–Ci response: photosynthesis in the phenomic era. Wiley Online Library,

Taylor SH, Long SP (2017) Slow induction of photosynthesis on shade to sun transitions in wheat may cost at least 21% of productivity. Philosophical Transactions of the Royal Society B: Biological Sciences 372 (1730):20160543.

Tomás M, Flexas J, Copolovici L, Galmés J, Hallik L, Medrano H, Ribas-Carbó M, Tosens T, Vislap V, Niinemets Ü (2013) Importance of leaf anatomy in determining mesophyll diffusion conductance to CO2 across species: quantitative limitations and scaling up by models. Journal of experimental botany 64 (8):2269-2281.

Tosens T, Nishida K, Gago J, Coopman RE, Cabrera HM, Carriquí M, Laanisto L, Morales L, Nadal M, Rojas R, Talts E, Tomas M, Hanba Y, Niinemets Ü, Flexas J (2016) The photosynthetic capacity in 35 ferns and fern allies: mesophyll CO2 diffusion as a key trait. New Phytologist 209 (4):1576-1590.

Ubierna N, Gandin A, Boyd RA, Cousins AB (2017) Temperature response of mesophyll conductance in three C4 species calculated with two methods: 18O discrimination and in vitro Vpmax. New Phytologist 214 (1):66–80.

von Caemmerer S (2000) Biochemical models of leaf Photosynthesis. Thechniques in Plant Science. CSIRO Publishing, Collingwood

von Caemmerer S, Farquhar GD (1981) Some Relationships between the Biochemistry of Photosynthesis and the Gas-Exchange of Leaves. Planta 153 (4):376-387.

Figure S1. Alternative path dependent methods

Panel **A** shows the method of Björkman et al. (1980). The A/C_i curve for the treated plant (in red) is approximated with that of the healthy plant (in blue) for $C_i > C_{i\,op}$, translated vertically to match the operational assimilation of the measured plant as:

$$f(C,\boldsymbol{b}') \approx f(C,\boldsymbol{b}'') - \left[f\left(C_{i\,op},\boldsymbol{b}''\right) - f\left(C_{i\,op},\boldsymbol{b}'\right)\right], \qquad \text{S1}$$

where $\boldsymbol{b}'$ and $\boldsymbol{b}''$ are the set of parameters of the treated, and healthy plant, respectively; $f(C,\boldsymbol{b}')$ is the A/C function to be estimated; $f(C,\boldsymbol{b}'')$ is the known A/C function with the parameters $\boldsymbol{b}''$ determined for the healthy plant; the expression in square brackets is the down-translation (Figure 4A). A_{op} is the rate of assimilation of the treated plant in operational conditions, $f\left(C_{iop},\boldsymbol{b}'\right)$ in Eqn S1; $A_{Pot\,Ci}$, is the rate of assimilation that the healthy plant would have if C_i were that of the treated plant in the operational condition C_{iop},, $f\left(C_{iop},\boldsymbol{b}''\right)$ in Eqn S1; A_{Pot} is that a healthy plant would have in absence of stomatal barrier, $f(C_a,\boldsymbol{b}'')$ in Eqn S1. Limitations are evaluated by removing stomatal limitation first in the transition between state I and state II, and then by removing non-stomatal limitation in the transition between state II and state III. The conventional three point calculation (Bellasio et al. 2023) gives the same results as the current framework: the total stomatal contribution $\Xi(C_i)_A$ is $A_{Pot} - A_{Pot\,Ci}$, and the total non-stomatal contribution $\Xi(L_{NS})_A$ is $A_{Pot\,Ci} - A_{op}$. Calculation of Eqn S1 for each step of the first transition is shown in Sheet 8 of Workbook III.
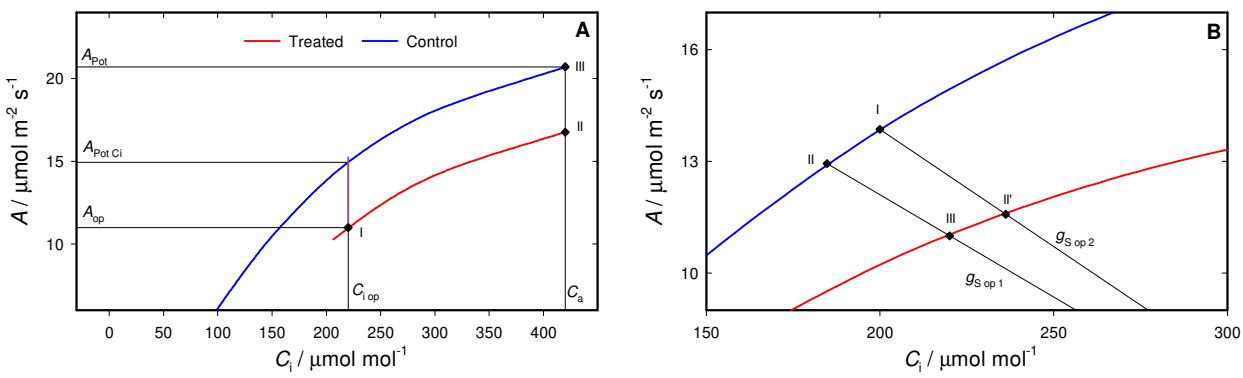
Panel **B** shows two path-dependent variants of contribution analysis where a healthy plant (in blue) undergoes a generic treatment that restrict assimilation (in red). State I and III represents a generic operational point of the treated plant, and healthy plant, respectively, while state II is an intermediate state through which the transition is assumed to occur. The first path assumes that in response to the treatment stomata respond before any change in leaf biochemical processes occurs, that is, a transition from state III to state II, with reduced g_S, and then to state I, with lower photosynthetic potential but equal g_S. The second variant assumes that biochemical regulation occurs before stomata respond, that is, a path through state II′ where g_S equals that of the healthy plant, while the parameterization corresponds to that of the treated plant. In the path 'stomata first' during the transition between state I and state II, $\Xi(g_S)_A$ was -1.1 µmol m^{-2} s^{-1}. In the path 'mesophyll first' during the transition between state II and state III, $\Xi(g_S)_A$ was -0.7 µmol m^{-2} s^{-1}. The calculations are in Sheets 9 and 10 of Workbook III.